

# Conducting Polymer Nanocomposites: The Role of the Electronic Fingerprints of Carbon Nanotubes

Pui Lam Chiu, Yufeng Ma, Arnaldo Serrano, Lin Wang, Richard Mendelsohn, Huixin He\*

\*Department of Chemistry, Rutgers University  
Room 216, 73 Warren Street, Newark, NJ 07102  
Phone: 973-353-1254; Fax: 973-353-1264  
Email: huixinhe@newark.rutgers.edu

## ABSTRACT

We report that dispersion and functionalization of single-walled carbon nanotubes (SWNTs) with different dispersing methods and dispersing agents result in different SWNTs with different electronic structures and surface functionalities. *In-situ* polymerizations of the monomers, 3-aminophenylboronic acid hemisulfate salt, in the presence of these various SWNTs, we obtained poly (aniline boronic acid) nanocomposites. The electronic and molecular structures of the poly (aniline boronic acid) in the composite and therefore the performance of the composite are very different, depending on the electronic fingerprints and the surface functionalities of the SWNTs.

**Keywords:** polyaniline, composite, self-doped, carbon nanotubes, electronic fingerprint

## 1 INTRODUCTION

Tremendous efforts have been made over the past decade to prepare polymer and carbon nanotube (CNT) composites with an aim to synergistically combine the merits of each individual component [1-6]. *In-situ* polymerization of the respective monomers in the presence of carbon nanotubes is expected to form genuine CNT-polymer composites with much more enhanced functions compared to the "post mixing" approaches [5-7]. *In-situ* polymerization requires pre-dispersing the carbon nanotubes into solution. Different dispersion approaches result in carbon nanotubes with different surface chemistries and electronic structures. The expected improvement in the nanocomposites is critically dependent on the polymer-nanotubes interfacial chemical and electronic interactions. However, the impacts of dispersion and functionalization of the carbon nanotubes on the process of fabricating nanocomposites and the molecular structure of the polymer in the composite has not yet been extensively addressed.

In our previous report [8], a water-soluble self-doped polyaniline (polyaniline boronic acid) nanocomposite was fabricated by the *in-situ* polymerization of 3-aminophenylboronic acid salt monomers in the presence of single-stranded DNA-dispersed and functionalized carbon nanotubes (ss-DNA-SWNTs). We found that the

dispersion and functionalization of SWNTs with ss-DNA d(T)30 dramatically changed the molecular structure and properties of the polymer in the nanocomposite. The results showed that the ss-DNA-SWNTs acted as active stabilizers, which were capable of reducing the polyaniline backbone from the unstable, degradable, and fully oxidized pernigraniline state to the more stable and conducting emeraldine state due to their reductive ability, which improved the chemical stability of the polymer. We also found that the rate of the polymerization was greatly increased.

In this work, we report the fabrication of poly (aniline boronic acid) (PABA) nanocomposite by chemical polymerization of 3-aminophenylboronic acid hemisulfate salt in the presence of SWNTs with various electronic structures and surface functionalizations. From Ultraviolet-Visible-Near Infrared (UV-Vis-NIR) and Fourier Transform Infrared (FT-IR) spectroscopic studies of these composites, we found the molecular and electronic structures of the PABA in these nanocomposites were very different. We believe that these dramatic differences are due to different electronic structures and the surface functionalities of the SWNTs, which give rise to different interactions with the ABA monomers before, during and after the polymerizations.

## 2 EXPERIMENTAL SECTION

### 2.1 Materials

HiPco Purified SWNTs were purchased from Carbon Nanotechnologies, Inc. Single-stranded DNA (ss-DNA) with d(T)30 was purchased from Integrated DNA Technologies. 3-Aminophenylboronic acid hemisulfate salt, potassium fluoride (KF) and all other chemicals were used as received from Aldrich Chemicals, Inc. Chitosan (CHIT), with a molecular weight of  $1.3 \times 10^6$ , was purchased from Spectrum Chemicals, Inc. All solutions were prepared using nanopure water (18.2 M $\Omega$ ) (Nanopure water, Barnstead). All samples after polymerization and before any type of characterization were rinsed and cleaned with the same nanopure water.

## 2.2 Dispersion and Functionalization of SWNTs

SWNTs were dispersed into water using the method described by Zheng et al [9], resulting in ss-DNA-dispersed nanotube solutions at high concentrations. The dispersed ss-DNA-SWNT was further centrifuged three times to remove the insoluble materials and was dialyzed to remove free ss-DNA, resulting in pure ss-DNA-SWNT.

The detailed procedure to disperse and functionalize SWNTs with CHIT is as follows: a 0.5 wt. % chitosan solution was prepared by dissolving the proper amount of CHIT in 0.05 M H<sub>2</sub>SO<sub>4</sub> aqueous solution at about 85°C. The solution was then cooled to room temperature. 3 mL of 1 mg·mL<sup>-1</sup> of SWNTs was prepared in the CHIT stock solution, and was sonicated in an ice-bath for 1.5 hours to complete the dispersion. The chitosan-dispersed and functionalized carbon nanotubes (CHIT-SWNTs) were purified by following the procedures as stated above.

Microwave assisted-functionalized SWNTs (MF-SWNTs) in solid state were dissolved in nanopure water, forming a stock MF-SWNT solution (6.87 mg/mL). All solutions that required MF-SWNTs were prepared using this stock solution. The detailed procedure for dispersing MF-SWNT is described in a recent report by Wang et al. [10].

## 2.3 In-situ Fabrication of SWNT-Poly (aniline boronic acid) Nanocomposites

A typical synthetic procedure for the preparation of an aqueous solution of SWNTs-PABA nanocomposites is as follows: 2.5 mM of 3-aminophenylboronic acid hemisulfate salt (ABA) and 40 mM of potassium fluoride (KF) were dissolved in 0.5 M H<sub>2</sub>SO<sub>4</sub>. 6.4 mg of different types of SWNTs were then added to the prepared monomer solutions. The final volumes of all the solutions above were exactly 3.0 mL. The solutions were purged with nitrogen for 30 – 45 minutes in ice-baths to remove the dissolved oxygen in the solutions. The chemical polymerization of ABA was initiated by adding 0.0375 M ammonium persulfate, (NH<sub>4</sub>)<sub>2</sub>S<sub>2</sub>O<sub>8</sub> (APS) (also in 0.5 M H<sub>2</sub>SO<sub>4</sub>) as an oxidant to the mixture at a rate of one drop every 20 minutes. The polymerization was carried out at 0°C with nitrogen purging until the reaction stopped. Control experiments were also performed to fabricate neat poly (aniline boronic acid) (PABA) under the same conditions, except the additions of different types of SWNTs.

## 2.4 Ultraviolet-Visible-Near Infrared (UV-Vis-NIR) and Fourier Transform Infrared (FT-IR) Spectra

All UV-Vis-NIR absorption spectra were obtained using a Cary 500 UV-Vis-NIR Spectrophotometer with double

beam mode with the range of 200-1400 nm. FT-IR spectra were measured on a Spectrum Spotlight FT-IR Imaging System (Perkin Elmer Instruments). The aqueous solutions of the neat PABA and the nanocomposites of PABA with different types of SWNTs; fabricated at 0°C, were left undisturbed for 6 hours to let the polymer settle. The acidic supernatant was carefully pipetted out and the neat polymer and the composites were washed with and re-dispersed into 18.2 MΩ nanopure water. This procedure was repeated three times to remove the sulfuric acid, the monomers and other impurities remaining in the solutions. Thin films of neat PABA and composites were prepared on a calcium fluoride (CaF<sub>2</sub>) substrate from the respective purified PABA solutions. All FT-IR spectra were obtained with the range of 750 – 1700 cm<sup>-1</sup> with 2 cm<sup>-1</sup> spectral resolutions.

## 3 RESULTS AND DISCUSSION

### 3.1 Electronic Fingerprints and Surface Functional Groups of the SWNTs

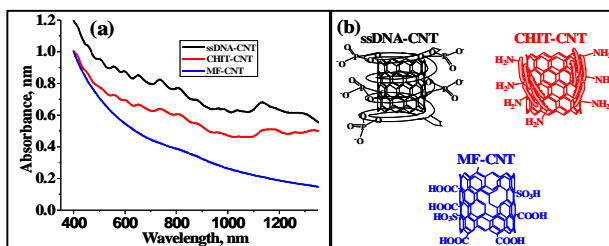


Figure 1. (a) UV-Vis spectra of (black) ss-DNA-CNT; (Red) CHIT-CNT; (Blue) MF-CNT. All the carbon nanotube solutions were at pH 1 (with nitrogen purging). (b) Various SWNTs with the surface chemistries shown.

UV-Vis-NIR electronic absorption spectroscopy was used to study the electronic structures of the SWNTs dispersed and functionalized with different dispersing agents and methods. Figure 1 shows UV-Vis-NIR spectra of ss-DNA-SWNTs, CHIT-SWNTs and MF-SWNTs. Well-resolved and narrow peaks appear in the spectra of ss-DNA-SWNTs, CHIT-SWNTs, but not the MF-SWNTs. It is reported that well-resolved and narrow peaks in a UV-Vis-NIR spectra of SWNTs are attributed to the interband transitions between van Hove singularities in the density of states (DOS) of individual SWNTs. The appearance of the peaks suggests that SWNTs exist as individual and/or very small bundles, and also that the intrinsic properties of the SWNTs remain intact. These results demonstrate that ss-DNA (black) and CHIT (red) have the ability to disperse the SWNTs into aqueous solutions with the intrinsic electronic properties of SWNTs intact, which is in agreement with previous reports. Zheng et al [9], reported that single-stranded DNA was able to effectively disperse nanotubes into aqueous solution, resulting in ss-DNA helically wrapped-carbon nanotubes with both negatively charged phosphate groups and bare graphite regions exposed to the solution as shown in Figure 1b (black). It

was reported that after CHIT dispersed the SWNTs, CHIT wraps around the SWNTs with positively charged amine groups exposed to aqueous solution [11], as shown in Figure 1b (red). However, the UV-Vis-NIR absorption spectrum of MF-SWNTs does not show the transition bands of SWNTs (Figure 1a, blue). This indicates that the intrinsic properties of SWNTs are lost. As reported before, MF-SWNTs was functionalized with extensive amounts of  $-COOH$  and  $-SO_3H$  groups on the surfaces, with one out of three carbon atoms that are carboxylated and one out of ten that is sulfonated [10].

### 3.2 Electronic and Molecular Structures of PABA in SWNT Composites

UV-Vis-NIR absorption spectra have been widely used to determine the oxidation states of polyaniline because of their distinct chromatic properties. To study the impact of the electronic structures and surface functionalities of the SWNTs on the electronic structures of polyaniline in SWNT composites, we fabricated the composites by in-situ polymerization of ABA in the presences of various SWNTs at  $0^\circ C$ . The final products are characterized with UV-Vis-NIR and FT-IR spectroscopies.

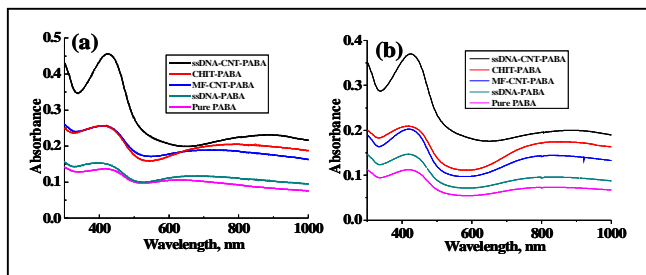


Figure 2. UV-Vis absorption spectra of (a) Pure PABA and different SWNTs-PABA composites before treatment of  $NaBH_4$ ; (b) Pure PABA and different SWNTs-PABA composites after treatment of  $NaBH_4$

Figure 2a shows the UV-Vis-NIR spectra of the various composites polymerized at  $0^\circ C$  for 12 hours. For comparison, the spectra of neat PABA and PABA polymerized in the presence of ss-DNA are also displayed. Since the concentration of ssDNA used was the same as that of ssDNA-SWNTs, the spectra clearly demonstrate that roles of ssDNA and SWNT on the properties of PABA. In each spectrum, two broad peaks appear. The maxima at around 400 nm can be assigned to the  $\pi-\pi$  transitions and the corresponding wavelengths for all composites are similar to each other. However, the peak positions at longer wavelengths are different depending on the presence or absence of SWNTs, and on the presence of various SWNTs during the polymerization. The peaks at 625 nm, 670 nm, 713 nm, 780 nm, and 890 nm correspond for pure PABA, ss-DNA-PABA, MF-CNT-PABA, CHIT-CNT-PABA, and ss-DNA-CNT-PABA, respectively. The peaks in this wavelength region have been assigned to aromatic-

quinoid transition in pernigraniline, or polaron and delocalized bipolaron structures in the conductive, partially oxidized emeraldine salt states. These results lead to the conclusion that the pure PABA exists more in the degradable, fully oxidized pernigraniline state, while the PABA in the composites exist in the more conductive and stable emeraldine state. Depending on the electronic structures and surface functionalities of the SWNTs, the amounts of emeraldine and pernigraniline in the composites are different. With the intact intrinsic electronic structures, and negatively charged ss-DNA-SWNTs, most of the PABAs in the composites exist in the conductive and stable emeraldine state. With the destroyed intrinsic electronic structures during the dispersion and negatively charged surface of MF-SWNT, the PABA existed more in the degradable pernigraniline state. With the intrinsic electronic structure remained and positively charged CHIT-SWNTs, the amount of PABA exists in the emeraldine state is less than that of ss-DNA-SWNTs but more than that of MF-SWNTs.

To further support this conclusion, we reduced the pure PABA and composites with  $NaBH_4$  [6]. Figure 2b shows the UV-Vis-NIR absorption spectra of the materials after reductions with  $NaBH_4$ . The peaks red shifted 195 nm, 150 nm, 97 nm, 60 nm, and 4 nm for pure PABA, ss-DNA-PABA, CHIT-CNT-PABA, MF-CNT-PABA and ss-DNA-CNT-PABA, respectively. It is obvious that the extent of the red shifts by  $NaBH_4$  reduction are closely related to the electronic structures and surface functional groups of the SWNTs, providing further support for the conclusion described above. After reduction, the pure PABA still absorbs at a shorter wavelength than the composites. It is possible that the polyaniline backbone has different conjugated structures in the composite depending on the SWNTs.

To understand the molecular structures of the neat PABA and the SWNTs-PABA composites, we also used FT-IR spectroscopy to examine polymer films prepared from the respective solutions. Figure 3 shows the FT-IR spectra for the PABA and the composites prepared with different SWNTs.

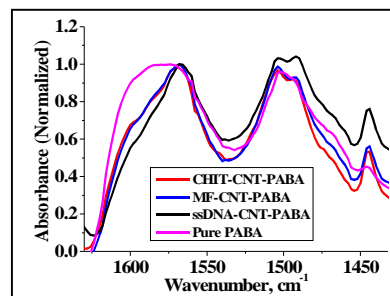


Figure 3. FT-IR spectra of pure PABA and the PABA composites with different SWNTs.

All the spectra exhibit absorption of the characteristic  $C=C$  stretching vibrations of the benzenoid ring at  $1444\text{ cm}^{-1}$ , and of the quinoid ring at  $1568\text{ cm}^{-1}$ . The ratio of the

relative intensities of quinoid to benzenoid ring modes ( $I_{1568}/I_{1444}$ ) in the neat PABA is 14.0, which suggests that the amount of quinoid units is larger than the benzenoid units in the neat PABA films. This is consistent with what we previously reported that most of the PABAs in the neat polymer exist in the pernigraniline state. The ratios of different composites were calculated to be 2.71, 2.82 and 4.14 for ss-DNA-CNT-PABA, CHIT-CNT-PABA and MF-CNT-PABA, respectively. The ratios in the composites are surprisingly low, which indicates that the relative amounts of quinoid units decreased and benzenoid units increased in the PABA backbones when polymerized in the presence of SWNTs. The amount of the quinoid units decreases from ss-DNA-CNT-PABA to CHIT-CNT-PABA to MF-CNT-PABA. These results further conclude that most of the PABA in the neat PABA exists in the fully oxidized pernigraniline state and most of the PABA in the ss-DNA-SWNT-PABA composite exists in the stable emeraldine state. Another interesting feature observed in the FT-IR spectrum is that the neat PABA exhibits a broad peak at  $1568\text{ cm}^{-1}$ . In contrast, the composites show relatively sharp absorption peaks at  $1568\text{ cm}^{-1}$  and shoulders at  $1600\text{ cm}^{-1}$ . The intensities of the shoulders increase from ss-DNA-SWNT-PABA, to CHIT-SWNT-PABA, to MF-SWNT-PABA. It was reported that these shoulder peaks attributes to phenazine-like structures in the PABA backbone, suggesting that more branched structures were produced in neat PABA. Although all the SWNTs show the abilities to prevent branched structure formation, their efficiencies can be ranked in descending order: ss-DNA-SWNTs, CHIT-SWNTs, and MF-SWNTs. This trend is also consistent with the changes of the ratios of  $I_{1568}/I_{1444}$  in the different composites. The changes of the peak positions in the UV-Vis-NIR absorption spectra, and the extents of the red shifts of this peaks after  $\text{NaBH}_4$  treatment also follow the trend above. Therefore we can conclude that ss-DNA-SWNTs, with their intrinsic electronic properties intact and negatively charged surface, are the most effective in facilitating the fabrication of conductive and stable PABAs, which exist in the emeraldine state. These PABAs also have less branched and longer conjugated structures. For MF-SWNTs, with their intrinsic electronic structure destroyed during the process of dispersion, even though the surface of the MF-SWNTs is negatively charged, are the least effective in fabricating high-quality PABA. With their intrinsic electronic properties intact, but with a positively charged surface, the CHIT-SWNTs are more efficient than MF-SWNTs, but not as efficient as ss-DNA-SWNTs in fabricating conducting and long-conjugated PABAs.

In summary, we studied the molecular and electronic structures of PABA in the composites fabricated in the presence of different SWNTs. The results demonstrate that the electronic fingerprints and the surface functionalities of the SWNTs greatly impact the molecular structures and therefore the performance of the fabricated composites.

## REFERENCES

- [1] S. Iijima, *Nature*, 354, 56, 1991.
- [2] P. M. Ajayan; O. Stephan; C. Colliex, D. Trauth, *Science*, 265, 1212, 1994.
- [3] L. Dai, W. H. A. Mau, "Controlled Synthesis and Modification of Carbon Nanotubes and C60: Carbon Nanostructures for Advanced Polymeric Composite Materials," *Adv. Mater.*, 13, 899-913, 2001.
- [4] H. Zengin; W. Zhou, J. Jin, R. Czerw, J. D. W. Smith, L. Echegoyen, D. L. Carroll, S. H. Foulger, J. Ballato, "Carbon Nanotube Doped Polyaniline," *Adv. Mater.*, 14, 1480-1483, 2002.
- [5] M. Cochet; W. K. Maser; A. M. Benito; M. A. Callejas, M. T. Martínez, J. M. Benoit, J. Schreiber, O. Chauvet, "Synthesis of a New Polyaniline/Nanotube Composite: "in-situ" Polymerisation and Charge Transfer through Site-Selective Interaction," *Chem. Comm.*, 1450, 2001
- [6] R. Sainz, A. M. Benito, M. T. Martínez, J. F. Galindo; J. Sotres, A. M. Baró, B. Corraze; O. Chauvet, W. K. Maser, "Soluble Self-Aligned Carbon Nanotube/Polyaniline Composites," *Adv. Mat.*, 17, 278-281, 2005.
- [7] X. H. Li, B. Wu; J. E. Huang, J. Zhang, Z. F. Liu; H. L. Li, "Fabrication and Characterization of Well-Dispersed Single-Walled Carbon Nanotube/Polyaniline Composites." *Carbon*, 411, 1670-1673, 2002.
- [8] Y. F. Ma, S. R. Ali; L. Wang, P. L. Chiu, R. Mendelsohn; H. X. He, "*In-situ* Fabrication of A Water-Soluble, Self-Doped Polyaniline Nanocomposite: the Unique Role of DNA Functionalized Single-Walled Carbon Nanotubes," *J. Am. Chem. Soc.*, 128, 12064-12065, 2006.
- [9] M. Zheng, A. Jagota, E. D. Semke; B. A. Diner, R. S. Mclean; S. R. Lustig; R. E. Richardson, N. G. Tassi, "DNA-assisted Dispersion and Separation of Carbon Nanotubes," *Nat. Mater.*, 2, 338-342, 2003.
- [10] Y. Wang, Z. Iqbal, S. Mitra, "Rapidly Functionalized, Water-Dispersed Carbon Nanotubes at High Concentration," *J. Am. Chem. Soc.*, 128, 95-99, 2006.
- [11] H. Yang; S. C. Wang; P. Mercier, D. L. Akins, "Diameter-Selective Dispersion of Single-Walled Carbon Nanotubes Using a Water-Soluble, Biocompatible Polymer," *Chem. Commun.*, 1425-1427, 2006.